Accepted Manuscript

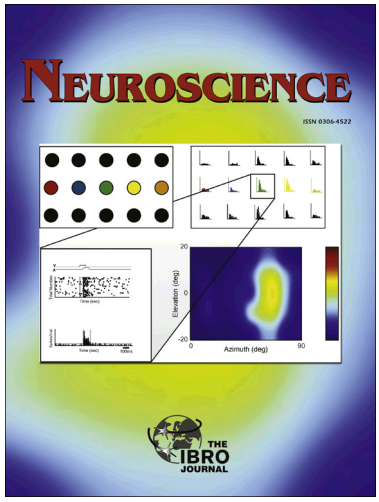

Differential recruitment of brain networks during visuospatial and color processing: evidence from ERP microstates

Ingrida Antonova, Anja Bänninger, Thomas Dierks, Inga Griskova-Bulanova, Thomas Koenig, Axel Kohler

PII: S0306-4522(15)00705-8
DOI: http://dx.doi.org/10.1016/j.neuroscience.2015.07.078
Reference: NSC 16475

To appear in: *Neuroscience*

Accepted Date: 28 July 2015

Please cite this article as: I. Antonova, A. Bänninger, T. Dierks, I. Griskova-Bulanova, T. Koenig, A. Kohler, Differential recruitment of brain networks during visuospatial and color processing: evidence from ERP microstates, *Neuroscience* (2015), doi: http://dx.doi.org/10.1016/j.neuroscience.2015.07.078

Differential recruitment of brain networks during visuospatial and color processing: evidence from ERP microstates

Abbreviated Title: Cortical dynamics of visuospatial processing

*Ingrida Antonova [1, 2], *Anja Bänninger [1], Thomas Dierks [1], Inga Griskova-Bulanova [2], Thomas Koenig [1], Axel Kohler [3]

(1) Translational Research Center, University Hospital of Psychiatry, University of Bern, Bolligenstrasse 111, CH-3000 Bern 60, Switzerland

(2) Department of Neurobiology and Biophysics, Vilnius University, Ciurlionio 21/27, LT-03101, Vilnius, Lithuania

(3) Institute of Cognitive Science, University of Osnabrück, Albrechtstrasse 28, D-49076 Osnabrück, Germany

*equal contribution

Correspondence to: I. Antonova

Present address: Translational Research Center, University Hospital of Psychiatry, University of Bern, Bolligenstrasse 111, CH-3000 Bern 60, Switzerland

E-mail address: ingrida.antonova@gmail.com

The authors declare no conflict of interest

Abstract

Recent functional magnetic resonance imaging (fMRI) studies consistently revealed contributions of fronto-parietal and related networks to the execution of a visuospatial judgment task, the so called “Clock Task”. However, due to the low temporal resolution of fMRI, the exact cortical dynamics and timing of processing during task performance could not be resolved until now. In order to clarify the detailed cortical activity and temporal dynamics, 14 healthy subjects performed an established version of the “Clock Task”, which comprises a visuospatial task (angle discrimination) and a control task (color discrimination) with the same stimulus material, in an electroencephalography (EEG) experiment. Based on the time-resolved analysis of network activations (microstate analysis), differences in timing between the angle compared to the color discrimination task were found after sensory processing in a time window starting around 200 ms. Significant differences between the two tasks were observed in an analysis window from 192 ms to 776 ms. We divided this window in two parts: an early phase – from 192 ms to ~ 440 ms, and a late phase – from ~ 440 ms to 776 ms. For both tasks, the order of network activations and the types of networks were the same, but, in each phase, activations for the two conditions were dominated by differing network states with divergent temporal dynamics. Our results provide an important basis for the assessment of deviations in processing dynamics during visuospatial tasks in clinical populations.

Keywords: microstate analysis; visuospatial judgment; EEG; ERP; parietal cortex; frontal cortex

INTRODUCTION

The scientific study of spatial cognition dates back at least to the late 17th century when Descartes (in his Treatise of Man, 1662), with his theory of a "natural geometry", reflected on the problem of how the brain processes the third dimension for the perception of distance (Marshall and Fink, 2001). The processing of visuospatial information is considered crucial for interacting effectively with our environment, even if we are mostly unaware of the process itself. The impact of an impaired processing is, for example, evident in Alzheimer's disease, where early symptoms include, among others, impoverished visuospatial skills (Arnáiz and Almkvist, 2003; Thulborn, et al., 2000). An impairment of visuospatial skills was also observed in schizophrenia (Bourque et al., 2013; Bustillo et al., 1997; Cavézian et al., 2011; Hardoy et al., 2004; Leiderman and Strejilevich, 2004; McCourt et al., 2008; Zhai et al., 2011).

With the emergence of lesion studies and more recently functional brain imaging techniques, it was possible to investigate the neural networks and anatomical substrates involved in the processing of visuospatial information. Due to this progress, it is nowadays well confirmed that the human parietal cortex is activated during the performance of visuospatial tasks (Colby and Goldberg, 1999; Culham and Kanwisher, 2001; Dierks et al., 1999; Formisano et al., 2002; Haxby et al., 1991; Husain and Nachev, 2007; Marshall and Fink, 2001; Mesulam, 1999; Newcombe et al., 1987; Schicke et al., 2006; Trojano et al., 2000). In their review, Culham and Kanwisher (2001) point out that the investigation of human parietal cortex, excluding somatosensory regions, is challenging since they belong to the functional category of "association cortex" with rather complex, multimodal responses. The authors are referring to human and monkey studies which found activations of the parietal lobes in a variety of tasks involving, among others, visuomotor control, attention, eye

movements, spatial and non-spatial working memory, mental imagery and task switching. Regarding hemispheric asymmetries, a preferentially right-parietal involvement during visuospatial processing (Corballis, 2003; Sack et al., 2002b), implicit learning of visual feature combinations (Roser et al., 2011) and visuospatial attention (Hilgetag et al., 2001; Müri et al., 2002; Shulman et al., 2010) has been revealed. As Corballis (2003) states, research with callosotomy (or "split-brain") patients demonstrated that the strict dichotomy in a left-hemispheric specialization for controlling actions and linguistic processes and a right hemispheric specialization for visuospatial processing is oversimplified. The hemispheric asymmetries are likely to arise at higher levels of visual processing whereby the right hemisphere can be described as more "visually intelligent" than the left hemisphere (Corballis, 2003). An example of higher-order visuospatial processing is visuospatial judgment, which can involve the analysis of spatial relations, between stimulus parts or aspects of visual images, or more specifically spatial features of visual stimuli such as distances or angles (de Graaf et al., 2010).

A number of studies have used different versions of a specific visuospatial judgment task, the so called "Clock Task", to further elucidate the neural correlates underlying its processing. One frequently used version of the "Clock Task" consists of two conditions: a visuospatial-judgment condition, where participants have to evaluate the size of angles between two clock hands, and a non-spatial control condition, where participants have to discriminate the color of the clock hands while ignoring angle size. Sack et al. (2002a) addressed the question of functionality of the parietal cortex using this task. They could demonstrate with repetitive transcranial magnetic stimulation (TMS) that the parietal cortex (more precisely the superior parietal lobule, SPL) is of functional relevance for the execution of the "Clock Task". A later study using simultaneous functional magnetic resonance imaging (fMRI), TMS and behavioral measures, showed that both angle and color discrimination resulted in increased neuronal activity in parietal and frontal regions of both hemispheres, but

that only right but not left parietal TMS (of the SPL) resulted in significantly impaired behavioral performance (significant increase of mean reaction time) in the angle but not the color task (Sack et al., 2007). In another sequence of investigations, task difficulty was studied as a modulating factor of cortical activity during the "Clock Task". In these studies, only the visuospatial-judgment condition was used, where participants were asked to evaluate the size of angles between clock hands. In addition, the length of clock hands was varied to produce different levels of task difficulty (Vannini et al., 2004). With event-related fMRI, an association between the increase of neuronal activation – measured by the amplitude and spatial extent of the blood-oxygenation-level-dependent (BOLD) signal – in response to the increase of task demand was revealed in the right and left SPL (Vannini et al., 2004).

In addition to TMS interference effects, Sack and colleagues (2007) found that, during execution of visuospatial judgments, functional connectivity was enhanced between right SPL, right postcentral gyrus and right middle frontal gyrus. Following up on these results, two studies tested the causal relevance and time course of contributions from these candidate areas using TMS and fMRI effective connectivity. The contribution by middle-frontal sites could be confirmed by both methods, although the proposed processing sequence was inconsistent for the two approaches (de Graaf et al., 2009; de Graaf et al., 2010). The fMRI effective-connectivity results were pointing to a directed influence from frontal to parietal cortex, but the timing of TMS effects was similar for both, parietal and frontal sites.

So far, the "Clock Task" has not been investigated using electroencephalography (EEG). fMRI has high spatial resolution and has been frequently used when investigating the "Clock Task". However, due to the low temporal resolution of fMRI, the temporal dynamics of the networks involved in the Clock task have not been resolved until now. EEG and event-related potential (ERP) techniques have, in contrast to fMRI, the advantage to reveal neural dynamics with high temporal resolution. Moreover, particular methods such as microstate analysis (Murray et al., 2008) allow to explore and compare the activation of cortical

networks by precisely quantifying temporal features such as onset time or duration between conditions and groups. New insights into the precise timing of visuospatial processing might have practical implications for developing new screening procedures in relevant populations.

What type of clinically relevant information may we expect from microstate analysis? As previous fMRI studies (de Graaf et al., 2010; Sack et al., 2002a) reported, both the "Angle" and the "Color" task activated mostly overlapping areas, and significant differences in the strength of activation were found only in some of these areas that are more specific to a certain task performance. This could mean that BOLD differences of activation in the task specific areas occurred because of a difference in the number of neurons activated and/or due to a difference in the duration of activation. If BOLD differences occurred due to a larger number of neurons firing at the same time, this would increase the GFP of a microstate, and indicate a higher efficiency. If BOLD differences occurred due to a longer activation of particular brain areas, this would affect the duration of the corresponding microstate, and could indicate more difficulties with the particular information processing step. Previous fMRI studies (Prvulovic et al., 2002) using the Clock Task reported differences in functional activation between healthy participants and Alzheimer's disease patients. They found overlapping networks engaged in angle discrimination in both groups with more activity in the superior parietal lobule in healthy group and more activity in occipitotemporal cortex in the patient group. The authors assumed that a visuospatial processing dysfunction in the patient group occurred due to an atrophy of the superior parietal lobule with accompanying compensatory processing in other brain areas.

Temporal dynamics could play a crucial role in visuospatial processing and its' impairment. In contrast to low temporal resolution methods like fMRI, high temporal resolution EEG techniques allow registering brain activity changes in time, and microstate analysis allows to compare differences in the onsets, durations, and strength of network activations during particular processing steps between conditions and groups. Findings on the

temporal dynamics of visuospatial processing could be important for a better understanding of network activations and more nuanced interpretation of fMRI results. The description of network dynamics in samples of healthy participants could be an important reference for clinical studies allowing to identify affected processing stages during visuospatial analysis.

We applied microstate analysis to find, evaluate and compare components of the ERP evoked by two different discrimination tasks within the "Clock task" paradigm – the Angle discrimination task, and the Color discrimination task. If there are differences in temporal dynamics between two tasks, microstate analysis can capture these differences and quantify them statistically in terms of strength of activation. Therefore, this study aimed to use one of the established "Clock Tasks" in an EEG setting to gain novel insights into the neural underpinnings of visuospatial judgment.

EXPERIMENTAL PROCEDURES

Participants

Fourteen healthy subjects (4 men, 10 women), aged from 23 to 34 (Mean = 26.8 years, SD = 3.3), participated in this study. According to a short version of the Edinburgh Handedness Inventory, they were all right handed with a mean Laterality Quotient (L.Q., for calculation see Oldfield, 1971) of 86.7 (SD = 15.5), had normal or corrected-to-normal vision and no past history of neurological or psychiatric disorders. Subjects were asked to refrain from caffeine and nicotine use for at least four hours before their EEG session and they reported to be free of medication or drugs. The experimental procedure was approved by the local ethics committee and written informed consent was obtained before participation.

Stimuli

The same "Clock Task" as previously published (de Graaf et al., 2009, 2010; Sack et al., 2002a, 2007) was applied. Stimuli were created with CorelDraw, programmed for display with E-Prime Software (Version 2.0, Psychology Software Tools) and presented on an LCD monitor (HP L1950, 19-inch, height – 30 cm, width – 38 cm). The visual stimuli consisted of schematic analog clocks with a yellow face and two white or yellow hands presented on a black background. The angle between the clock hands varied in steps of 30° (for example stimuli see Fig. 1a). The task comprised an angle and color discrimination in which the visual stimuli were physically identical, but their task instructions differed. In the angle discrimination (ANGLE), targets were clocks with angles of 30° or 60° (small angles) and non-targets were clocks with angles of 90°, 120° or 150° (large angles). In the color

discrimination (COLOR), clocks with white hands were targets and clocks with yellow hands were non-targets. All stimuli and the fixation cross were equiluminant.

Task

Subjects were sitting comfortably on a chair in a darkened, sound-dampened and electrically shielded booth and a chin rest was used to avoid head movements. They were instructed to indicate via button press the detection of target (right index finger) and non-target (right middle finger) stimuli. Although the assignment of target and non-target to the stimulus categories was somewhat arbitrary, the participants were explicitly instructed to consider the deviant, small angles as target in the ANGLE task and the deviant white hands (compared to the yellow clock face) as target in the COLOR task. Our aim was to keep our tasks consistent with previous reference studies using the same task design (Sack et al., 2002, 2007). We also wanted to see whether the target/non-target instruction has a particular effect on brain activation, as time-resolved EEG allows a trial-based analysis in a complete factorial design. Most previous fMRI studies used a block design, where target and non-target trials were intermixed in single blocks.

For every trial, response time from stimulus onset until button press was measured. Both tasks were presented in a number of mini-blocks with 12 blocks per run (6 ANGLE and 6 COLOR blocks in alternating order). Prior to each block, a visual instruction cue (ANGLE or COLOR) was projected for 2000 ms. One block contained 10 stimuli, which were presented for 300 ms with pseudorandomized interstimulus intervals showing a white fixation cross (for experimental paradigm see **Fig. 1b**). Interstimulus intervals ranged from 2500 to 3500 ms in steps of 250 ms (equally distributed).

[insert **Fig. 1** about here]

Acquisition of EEG Data

For the EEG recording, equipment from EasyCap, Falk Minow (Herrsching, Germany) was used: The scalp EEG was recorded from 72 silver chloride ring electrodes mounted in an elastic cap and arranged in the extended International 10/20 system. Additionally, two electrooculogram electrodes (EOG) were applied for the detection of both horizontal and vertical eye movements. A Neurofax EEG-1100G system amplifier (Nihon Kohden, Tokyo, Japan) was connected to the cap and the EEG was referenced online with the left and right central electrodes C3 and C4 (all impedances were kept below 20 kΩ). The recording filters were set between 0.016 Hz and 120 Hz bandpass and the EEG was digitized with a sampling rate of 500 Hz.

Analysis of Behavioral Data

To analyze the behavioral data, the Predictive Analysis SoftWare (PASW Statistics, Version 18.0.0, Polar Engineering and Consulting) was used. The variables of interest were the reaction time (RT) of correctly answered trials and the accuracy of responses. A two by-two factorial repeated-measures analysis of variance (ANOVA) was used to assess main and interaction effects regarding RT and accuracy. The two factors for the analysis were “task” (angle versus color) and “stimulus” (target versus non-target). A five-by-two repeated-measures ANOVA was used to assess effects regarding RT of correctly answered trials in the Angle task with the factors “Size” (angle size) and “Hand” (clock hands color). This ANOVA was followed up by paired sample t-test analyses.

Analysis of ERP Data

The tool used for the basic analysis of the EEG data was Brain Vision Analyzer (Version 2.04, Brain Products, Munich). First, the EEG was corrected for eye movement artifacts by removing those components identified by an independent component analysis (ICA) which clearly accounted for vertical and horizontal eye movements. Then, epochs containing further artifacts were discarded in a semiautomatic artifact inspection applying criteria of a maximum allowed voltage step per sampling of 50 μV, a maximum difference of values in intervals of 200 ms of 500 μV, a maximum and minimum amplitude allowed of -200 μV to 200 μV and a check of low activity in intervals of 100 ms of 0.5 μV (maximum minus minimum). Channels containing a high amount of artifacts were replaced by linear interpolation between their neighboring electrodes, which was done for a total of 27 electrodes out of the 72 times 14 (=1008) traces. Thereafter, the data was recalculated to common average reference and then filtered (low cut off of 0.1 Hz to high cut off of 30 Hz). To define the optimal end of the time window for the analyses of EEG epochs, the distribution of reaction times from each subject were inspected; this resulted in a time window of 0 to 1000 ms from stimulus onset. Finally, averages of the epochs representing correctly answered trials were calculated separately for each subject and each of the four conditions (angle target, angle non-target, color target, color non-target, respectively), followed by the generation of grand means across all subjects of all four averaged conditions.

Test for consistent scalp topographies across subjects. To check whether across repeated measurements of the event-related scalp field data consistent topographies related to the experimental conditions could be revealed, a topographic consistency test (TCT, Koenig and Melie-García, 2010), which is based on nonparametric randomization techniques, was performed. The TCT is implemented in the open-source software Ragu (Randomization Graphical User interface; Koenig et al., 2011) based on Matlab (Version 7.6.0.324, R2008a, The MathWorks). The TCT has a significant impact on further analysis and interpretation of

the data because it allows limiting the data analysis window to periods where there is evidence for a constant set of neuronal sources (Koenig and Melie-García, 2010). As an index for the presence of a scalp field in the average across observations, the Global Field Power (GFP, Lehmann and Skrandies, 1980) is used. The GFP is "a single, reference-independent measure of response strength" (Murray et al., 2008) and can be mathematically equated to the standard deviation across all channels (Koenig and Melie-García, 2010). The procedure of the TCT was described by Koenig and Melie-García (2009, Chapter 8).

Microstate segmentation. By use of Ragu the event-related EEG data sets were segmented into representative topographic maps, the so called microstates. The concept of functional microstates was described first by Lehmann and colleagues (1987). Based on their observation that measured field configurations (being it spontaneous or evoked by a stimulus) remain stable for brief time periods before rapidly changing into another, often very different, configuration, they proposed that these microstates represent the basic building blocks of information processing (Brunet et al., 2011). As it is well established that different scalp field topographies are caused by different intracranial source activations (e.g. Vaughan, 1982), Koenig and Pascual-Marqui (2009, Chapter 7) pointed out that the analysis of microstates is particularly useful to explore differences in timing and amplitude of network activations. In ERP data, microstate analysis decomposes the data in a set of prototypical spatial components with presumably constant intracranial sources (and thus functions) that may vary systematically or randomly between conditions in their onset, time present, and strength.

In our study, the identification of microstate prototype maps, determination of the optimal number of microstates, and statistical analyses on microstate parameters was performed in Ragu (Koenig and Melie-García, 2010; Koenig et al., 2014). These three essential steps of the Ragu analysis are described in more detail below.

The identification of microstate prototype maps was based on the so-called AAHC (atomize and agglomerate hierarchical clustering) algorithm: In subsequent iterations, this algorithm re-combines the ERP topographies into topographic clusters in a way that the mean topography of these clusters maximizes the explained variance in the ERP data (Murray et al., 2008).

To define the optimal number of cluster maps, Ragu uses a cross-validation criterion (Koenig et al., 2014): Cross-validation computes microstate maps with different numbers of microstate classes based on ERPs averaged over a subset of the data (a learning set). These microstate maps and their timing are then applied to the remaining data (test set), and the variance explained by the microstate maps in this test set is computed as a function of the number of classes. The optimal number of microstates is selected where mean variance explained in the test set reaches a maximum. Based on this optimal number, the final microstate maps are computed using the entire data available (Koenig et al., 2014).

In Ragu, statistical analysis on microstate parameters is based on randomization statistics. Randomization statistics compares differences of particular microstate features between real data sets against the distribution under the null hypothesis. To calculate this distribution, grand means of ERP were calculated for four conditions (Angle target, Angle non-target, Color target, and Color non-target), and different features of the same microstates were compared between conditions. In order to obtain p values, a randomization (1000 times) procedure was used (Koenig and Melie-García, 2010; Koenig et al., 2014).

In order to investigate the timing of visuospatial processing during visuospatial judgement task, the onset, duration and amplitude (or the Area Under the Curve - AUC) of microstates were measured in four conditions (Angle target, Angle non-target, Color target, Color non-target) and compared using microstate analysis.

RESULTS

Behavioural results

RT and accuracy were averaged within subjects for each of the four conditions separately. Mean and standard deviations (SD) of RTs and accuracy for each condition are shown in **Table 1**. The two-by-two repeated-measures ANOVA regarding RT of correctly answered trials with factors "Task" (angle versus color) and "Stimulus" (target versus non-target) resulted in a significant main effect of the factor Task [F (1, 13) = 68.825, $p < 0.0001$]. Mean RTs were significantly shorter in the Color task as compared to Angle task (see **Table 1**). Neither a significant main effect of the factor Stimulus nor an interaction of both factors was obtained. Regarding accuracy of responses, the repeated measures ANOVA revealed a significant main effect of the factor Task [F (1, 13) = 6.896, $p < 0.02$] and a significant Task by Stimulus interaction [F (1, 13) = 18.528, $p < 0.001$]. Accuracy was significantly higher in the Angle task compared to the Color task, and an interaction could be explained by a lower accuracy in the Color Target condition compared to other conditions (**Table 2**), as was confirmed by paired samples T-test analysis of accuracy in four conditions. Note that the difference was only about 4 % between the Color Target (93 %) and the other conditions (> 97 %). No significant main effect of the factor Stimulus was obtained.

Table 1 Mean RTs and standard deviation (SD) for each condition:

	RT (ms)	SD	Accuracy	SD
Angle Target	717.83	78.263	0.973	0.0404
Angle Non-Target	730.88	74.779	0.975	0.0154
Angle mean	724.36	76.521	0.974	0.0279
Color Target	642.62	77.777	0.934	0.0803
Color Non-Target	653.88	85.137	0.970	0.0307
Color mean	648.25	81.457	0.952	0.0555

Table 2 p values and t values (in brackets) (df = 13) of paired sample T-test analysis of accuracy in four conditions:

	Angle Non-target	**Color Target**	**Color Non-target**
Angle Target	0.850 (0.193)	0.006 (3.321)	0.640 (0.479)
Angle Non-target	-	0.052 (2.134)	0.400 (0.870)
Color Target	-	-	0.031 (2.426)

Mean RTs and accuracy for each clock angle are shown separately in **Fig. 2**. The five-by-two repeated-measures ANOVA regarding RT of correctly answered trials in the Angle task with the factors "Size" (angle size) and "Hand" (clock hands color) resulted in a significant main effect of the factor Size [F (4, 52) = 32.511, p < 0.0001]. Neither a significant main effect of the factor Hands nor an interaction of both factors was obtained.

In the Angle task, as revealed by paired sample T-test analysis of angles (not separated by clock hands color), mean RTs for 60º and 90º angles were significantly longer compared to 30º, 120º, and 150º angles. Also, mean RT for 120º angle was significantly longer compared to a 30º angle (minimal t-value 3.4 (df = 27), all p-values below .002).

[insert **Fig. 2** about here]

[insert **Fig. 3** about here]

Microstates results

Waveshapes of four conditions were created for each electrode. Waveshapes for electrodes PO3, Pz, PO4, O1, Oz, and O2 are shown in **Fig. 3**. Waveshapes were not analyzed statistically, but were created to allow comparing the present data with other ERP papers.

TCT revealed that topographies were consistent across subjects in the entire analysis window between 0 and 1000 ms (except from 950 ms to 1000 ms in the Color non-target condition). The cross-validation of the optimal number of microstates reached a plateau after 10 clusters. The remaining analysis was thus based on 10 microstate classes (MS 1-10). Their respective topographies and times of presence are shown in **Fig. 4**.

[insert **Fig. 4** about here]

Visual inspection of microstates' timing and amount of activation (amplitude) revealed that the onsets of MS classes 1-4 were similar between the four conditions. Notable differences between the Angle and Color task appeared from 192 ms with the onset of MS 5, and persisted until MS 9. MS classes 5-9 differed between the Angle and Color task in their onset, duration and amount of activation (AUC). Also, differences between target and non-target stimuli appeared in the time window of these five MSs (192 – 776 ms), and as **Fig. 4** suggests, were most pronounced in the Angle task.

In more detail, the first MS class (MS 1) represents a baseline state in which visual cortical activity is not initiated yet. The next three MS classes (MS 2, MS 3, MS 4) represent early visual sensory processing. MS 2 corresponded by latency and topography to the P1 component, MS 3 was a transitional MS class, and MS 4 corresponded by latency and topography to the N1. MS classes 5-9 could be attributed by latency and topography to the P3. We were interested in later cognitive processing of visual stimuli, so statistical analysis was based on MS classes 5-9.

Values of onset, duration, and AUC for MS classes 5-9 are reported in **Table 3**. The onset, duration, and AUC of MS 5, MS 6, MS 7, MS 8 and MS 9 were chosen for statistical analysis. GFP was not reported, because AUC and duration account for GFP. Statistically significant differences between MS classes were observed from 192 ms to 776 ms. The main findings regarding the onset, duration, and AUC are reported below. For more details, see all p values of the overall analysis and post-hoc analysis in **Table 4**.

The main effect of "Stimulus" was observed only for the onset of MS 5 ($p = 0.003$) with an earlier onset for non-target as compared to target conditions. A similar tendency ($p = 0.054$) was observed for the onset of MS 6, where the onset for non-targets was earlier than for targets (see **Table 3** and **Table 4**).

In the analysis of the "Task" main effect, MSs 6 and 9 were "enhanced" during the Angle task and MSs 5, 7 and 8 during the Color task. In particular, main effects of Task were observed in MS 5 – 9 for duration and AUC, and in MS 6 (a tendency, $p = 0.054$), MS 7, and MS 9 for the onset. MS 6 and MS 9 had a significantly earlier onset for Angle compared to Color task, together with a significantly longer duration and higher amplitude (see **Table 3** and **Table 4**). Only MS 7 had a significantly earlier onset for Color task compared to Angle task ($p = 0.0001$). Finally, MS 5, MS 7, and MS 8 had significantly longer durations and higher amplitudes in the Color task compared to the Angle task (see **Table 3** and **Table 4**).

Significant interactions were observed in all five MSs for onset (except MS 7), duration (except MS 7), and AUC. The MS5 effects are based on slightly later onset of the "Angle Target" condition and longer duration and higher AUC of "Color Target" compared to the other conditions. For MS6, the onset of "Color Target" is later, and there is an especially large difference in duration and AUC for the "Target" conditions (Angle Target > Color Target). During MS7, AUC differs between the "Color", but not "Angle" conditions. Apart from minor onset variation, the MS8 effects derive from large duration and AUC differences between the Angle compared to the Color conditions. Finally, MS9 is characterized by a

specifically earlier onset and longer duration of "Angle Non-Target", with minor variations in AUC. All relevant post-hoc comparisons are summarized in **Table 4**.

Table 3 Onset, duration, and AUC values of MS classes 5-9 (analysis window 0 – 1000 ms):

MS class	Condition			
MS 5	Angle Target	Angle Non-target	Color Target	Color Non-target
Onset (ms)	200	192	198	196
Duration (ms)	42	44	66	42
AUC (ms*µV)	87.0	101.0	139.8	102.4
MS 6	Angle Target	Angle Non-target	Color Target	Color Non-target
Onset (ms)	242	236	264	238
Duration (ms)	112	94	56	78
AUC (ms*µV)	188.2	158.7	100.1	141.3
MS 7	Angle Target	Angle Non-target	Color Target	Color Non-target
Onset (ms)	354	330	320	316
Duration (ms)	88	102	118	124
AUC (ms*µV)	132.5	134.7	231.1	208.3
MS 8	Angle Target	Angle Non-target	Color Target	Color Non-target
Onset (ms)	442	432	438	440
Duration (ms)	72	10	156	146
AUC (ms*µV)	111.9	8.6	215.1	176.8
MS 9	Angle Target	Angle Non-target	Color Target	Color Non-target
Onset (ms)	514	442	594	586
Duration (ms)	264	290	96	108
AUC (ms*µV)	440.9	445.9	130.7	125.0

Table 4 p values of the overall and post-hoc statistical analysis of the onset, duration, and AUC of MS classes 5-9 (analysis window 0 – 1000 ms). Significant p values are indicated in

bold. Differences between measured values (>) are shown for significant p values and for almost significant tendencies:

MS class	Features	Overall analysis			Post-hoc analysis	
		Task	Stimulus	Interaction	Angle	Color
MS 5	Onset	1	**0.003 (T > NT)**	**0.015**	**0.016 (T > NT)**	0.76
	Duration	**0.021 (C > A)**	0.72	**0.0001**	0.82	**0.003 (T > NT)**
	AUC	**0.003 (C > A)**	0.67	**0.0001**	0.16	**0.007 (T > NT)**
MS 6	Onset	0.054 (C > A)	0.054 (T > NT)	**0.0001**	0.08	**0.006 (T > NT)**
	Duration	**0.0001 (A > C)**	0.71	**0.002**	**0.049 (T > NT)**	**0.03 (NT > T)**
	AUC	**0.0001 (A > C)**	0.8	**0.005**	**0.03 (T > NT)**	0.055 (NT > T)
MS 7	Onset	**0.0001 (A > C)**	0.09	0.17	0.016	0.55
	Duration	**0.0001 (C > A)**	0.3	0.07	0.057	0.28
	AUC	**0.0001 (C > A)**	0.54	**0.0001**	0.87	**0.02 (T > NT)**
MS 8	Onset	0.67	0.22	**0.046**	0.058 (T > NT)	0.79
	Duration	**0.0001 (C > A)**	0.69	**0.0001**	0.06	0.25
	AUC	**0.0001 (C > A)**	0.42	**0.0001**	**0.003 (T > NT)**	**0.004 (T > NT)**
MS 9	Onset	**0.0001 (C > A)**	0.56	**0.004**	**0.01 (T > NT)**	0.28
	Duration	**0.0001 (A > C)**	0.89	**0.004**	0.6	0.42
	AUC	**0.0001 (A > C)**	0.95	**0.004**	0.94	0.75

DISCUSSION

Brain areas and networks involved in the "Clock Task" are well known (de Graaf et al., 2009; de Graaf et al., 2010; Sack et al., 2002a; Sack et al., 2007), however, temporal dynamics of these networks activation are not clear yet. In order to answer this question, we applied the ERP technique and microstates analysis to establish the detailed temporal dynamics of cortical activity during the "Clock Task" visuospatial judgment and color judgment. We found that, although the same networks are generally active during all subtasks, there are major shifts in network recruitment in later time windows (> 200 ms).

The analysis of the behavioral data revealed a significant main effect of the factor "Task" regarding the reaction times of correctly answered trials. As Figure 2 and Table 1 depict, participants were faster in executing the color than the angle discrimination task. This result is in line with previous studies using the same version of the "Clock Task" (Sack et al., 2007; but see de Graaf et al., 2009, 2010, for balanced designs) and could be due to the existing mismatch of the ratio between target and non-target stimuli in the angle (2:3) compared to the color (1:1) task resulting in a facilitation of the latter. However, for comparability with previous research the same task was adopted in our current study.

The order of microstates did not differ between conditions, which may indicate that incoming information processing has to undergo the same steps, and only duration and strength of a particular topography can depend on the nature of the task. Therefore, no unique activation patterns, as one might expect for specialized and lateralized spatial analysis, were found. The first four microstates (MS 1-4) were similar in onsets across experimental conditions (Figure 4), which suggests that there is a high consistency of the early sensory information processing. MS 1 was considered to reflect a baseline state due to its occurrence

from 0 ms to 74-78 ms when the first ERP component (P1) appears. Other early MS classes (MS 2-4) reflected early visual sensory processing, because MS 2 corresponded by latency and topography to the P1, and MS 4 corresponded by latency and topography to the N1. The P1 and N1 components are attributed to early visual evoked potentials (VEP), because they are well known to be evoked by stimulus appearance, and can be modulated by features of visual stimuli (Butler et al., 2007; Foxe et al., 2001; Oka et al., 2001; Schechter et al., 2005), even if visual stimuli are viewed passively. These components can be modulated by selective attention and reveal differences of visuospatial information processing in simple tasks where spatial attention to lateralized visual stimuli is involved (Gomez Gonzalez et al., 1994; Hillyard and Anllo-Vento, 1998; Mangun and Hillyard, 1991).

However, the main interest of this study was in visuospatial judgment, which involves a cognitive processing of visuospatial information (de Graaf et al., 2010). Therefore, we were interested in later cognitive components. The first differences relating to this judgment in the context of the two different tasks occurred at 192 ms post stimulus. Thus, MS classes 5-9 were chosen to assess differences between conditions, resulting in a time window of interest from 192 to 776 ms.

Apart from minor differences in MS 5, the sequence of early cognitive components (MS 5-7) is characterized by a relative shift between MS 6 and MS 7 for the task conditions. MS 6 activation is more extensive and pronounced for the Angle and MS 7 activation for the Color condition. Interestingly, MS 7 offset is at about the same time (~440 ms) in all conditions, so RT differences cannot be explained by the relative emphasis of task-specific components in the early time window.

Differences are more pronounced in the late phase of cortical activity. MS 9 dominates the late cognitive component of processing during the Angle task and is much more extended in time presumably producing the RT increase for the Angle conditions. In the

Color task, MS 9 activation is limited to a small time window around button press. Otherwise, MS 8 activity during color processing is emphasized during the late cognitive phase.

Summing up these findings, we suggest that particular networks, represented by MS classes 5, 7, and 8 were more important for color information processing, whereas networks represented by MS classes 6 and 9 were more important for spatial information processing. In MS 5, 6, and 7, the strongest gradients were observed bilaterally over the parietal cortex, but gradients over frontal regions occurred in different places: MS 6 differed from others with widely distributed frontal negativity, and MS 7 had more positivity over the right hemisphere. MS 7 and MS 8 were significantly prolonged during the color judgment task.

In MS 8 and 9, the strongest gradients were observed over the right parietal cortex and weaker gradients over frontal regions, but the distribution of positive and negative activation was slightly different between microstates. These findings could be in line with fMRI data, where an increased activity in parietal and frontal regions was observed during execution of both tasks, as reported by Sack and colleagues (Sack et al., 2007).

As revealed by fMRI studies, the same cortical regions were active during both tasks, and only the strength of activation was different indicating task-specific regions: posterior parietal cortex (PPC) and middle frontal gyrus (MFG) for the "Angle" task; supramarginal gyrus (SMG), an anterior region of MFG (aMFG), and superior frontal gyrus (SFG) for the "Color" task (de Graaf et al., 2010). This observation is in line with our findings that showed the same microstates in both tasks. Though Prvulovic and colleagues (2002) used a different control task – clocks without hands – they reported similar results: They found overlapping networks activated by both visuospatial judgment and control tasks in healthy participants and Alzheimer's-Disease patients, but with less activity in the superior parietal lobule and more activity in occipitotemporal cortex in the patient group as compared to controls. Summing up these findings, one could thus suggest that both visuospatial and color processing have to undergo the same sequence of visual information processing steps, but

specific steps are prolonged if they are task-relevant and terminated quickly if not. In cases of impairment, visuospatial task-specific regions/steps could be affected and produce differences in duration and strength of activation from the healthy state or might even be replaced completely. The duration of microstates might thus be a feature of brain information processing that can, under normal circumstances, be adapted to particular environmental needs and that determines the depth of a particular information processing step. The investigation of microstates in clinical populations may thus be especially helpful to elucidate coping strategies, because only spatial differences in network activation are known but temporal dynamics were not established yet.

In comparison to previous fMRI studies, our EEG analysis allowed us to resolve the temporal dynamics of network states during visuospatial processing. Our findings provide a link between RT and network activations on a trial basis, leading to a more nuanced interpretation of existing and future fMRI studies.

Some limitations of the study design have to be mentioned. As described before, there is an existing mismatch of target to non-target stimuli between the angle (2:3) and the color (1:1) task. In our study, we decided to adhere to the specifications of previous studies in order to make the results comparable between experiments. For future studies, this mismatch should be corrected and task differences should be kept to a minimum. Reaction times show a differential pattern across the different stimulus classes. Color task RTs are relatively homogeneous, whereas the difficulty of angle discriminations is strongly affected by stimulus configuration. This might lead to merely quantitative differences in the recruitment of overlapping neural networks depending on task difficulty, as we observed in our EEG data.

Conclusions

Applying topographic techniques, significant differences in the timing of network activation between the angle and the color task including differences between target and non-target stimuli within each task were observed between 192 and 776 ms after stimulus onset: MS classes 5, 7, and 8 were more important for color information processing, whereas MS classes 6 and 9 were more important for spatial information processing. Activity gradients occurred over the same regions but topographic distribution of positive and negative activation differed between microstates. Moreover, differences in duration of the particular MS classes were significant between tasks. Thus, we conclude that the same areas are involved in both color and visuospatial processing but the timing and duration of this activation could be crucial for execution of the respective tasks. As visuospatial processing is, for example, impaired in Alzheimer's disease and schizophrenia, these insights might have practical implications by providing a basis for the development of new screening procedures.

Acknowledgements:

I. A. acknowledges support by the SCIEX-NMS Scientific Exchange Programme between Switzerland and the New Member States of the EU, Project 13.048.

REFERENCES

Arnáiz E, Almkvist O (2003) Neuropsychological features of mild cognitive impairment and preclinical Alzheimer's disease. Acta Neurologica Scandinavica 107(Suppl 179):34–41.

Bouque J, Lakis N, Champagne J, Stip E, Lalonde P, Lipp O, Mendrek A (2013) Clozapine and visuospatial processing in treatment-resistant schizophrenia. Cognitive Neuropsychiatry 18(6):615–630.

Brunet D, Murray MM, Michel CM (2011) Spatiotemporal analysis of multichannel EEG: CARTOOL. Computational Intelligence and Neuroscience, 2011:813–870.

Bustillo JR, Thaker G, Buchanas RW, Moran M, Kirkpatrick B, Carpenter WT Jr (1997) Visual information-processing impairments in deficit and nondeficit schizophrenia. Am J Psychiatry 154(5):647–654.

Butler PD, Martinez A, Foxe JJ, Kim D, Zemon V, Silipo G, Mahoney J, Shpaner M, Jalbrzikowski M, Javitt DC (2007) Subcortical visual dysfunction in schizophrenia drives secondary cortical impairments. Brain 130:417–430.

Cavézian C, Michel C, Rossetti Y, Danckert J, d'Amato T, Saoud M (2011) Visuospatial processing in schizophrenia: Does it share common mechanisms with pseudoneglect? Laterality: Asymmetries of Body, Brain and Cognition 16(4):433–461.

Colby CL, Goldberg ME (1999) Space and attention in parietal cortex. Annual Review of Neuroscience 22(1):319–349.

Corballis PM (2003) Visuospatial processing and the right-hemisphere interpreter. Brain and Cognition 53(2):171–176.

Culham JC, Kanwisher NG (2001) Neuroimaging of cognitive functions in human parietal cortex. Current Opinion in Neurobiology 11(2):157–163.

de Graaf TA, Jacobs C, Roebroeck A, Sack AT (2009) FMRI effective connectivity and TMS chronometry: complementary accounts of causality in the visuospatial judgment network. PLoS ONE 4(12):1–11.

de Graaf TA, Roebroeck A, Goebel R, Sack AT (2010) Brain network dynamics underlying visuospatial judgment: an FMRI connectivity study. Journal of Cognitive Neuroscience 22(9):2012–2026.

Dierks T, Linden DE, Hertel A, Günther T, Lanfermann H, Niesen A, Frölich L, Zanella FE, Hör G, Goebel R, Maurer K (1999) Multimodal imaging of residual function and compensatory resource allocation in cortical atrophy: a case study of parietal lobe function in a patient with Huntington's disease. Psychiatry Research 90(1):67–75.

Formisano E, Linden DEJ, Di Salle F, Trojano L, Esposito F, Sack AT, Grossi D, Zanella FE, Goebel R (2002) Tracking the mind's image in the brain I: time-resolved fMRI during visuospatial mental imagery. Neuron 35(1):185–194.

Foxe JJ, Doniger GM, Javitt DC (2001) Early visual processing deficits in schizophrenia: impaired P1 generation revealed by high-density electrical mapping. NeuroReports 12:3815–3820.

Gomez Gonzalez CM, Clark VP, Fan S, Luck SJ, Hillyard SA (1994) Sources of attention-sensitive visual event-related potentials. Brain Topography 7(1):41–51.

Hardoy MC, Carta MG, Catena M, Hardoy MJ, Cadeddu M, Dell'Osso L, Hugdahl K, Carpiniello B (2004) Impairment in visual and spatial perception in schizophrenia and delusional disorder. Psychiatry Reseach 127:163–166.

Haxby JV, Grady CL, Horwitz B, Ungerleider LG, Mishkin M, Carson RE, Herscovitch P, Schapiro MB, Rapoport SI (1991) Dissociation of object and spatial visual processing pathways in human extrastriate cortex. Proceedings of the National Academy of Sciences of the United States of America 88(5):1621–1625.

Hilgetag CC, Théoret H, Pascual-Leone A (2001) Enhanced visual spatial attention ipsilateral to rTMS-induced "virtual lesions" of human parietal cortex. Nature Neuroscience 4(9):953–957.

Hillyard SA, Anllo-Vento L (1998) Event-related brain potentials in the study of visual selective attention. Proc Natl Acad Sci 95:781–787.

Husain M, Nachev P (2007) Space and the parietal cortex. Trends in Cognitive Sciences 11(1):30–36.

Koenig T, Kottlow M, Stein M, Melie-García L (2011) Ragu: a free tool for the analysis of EEG and MEG event-related scalp field data using global randomization statistics. Computational Intelligence and Neuroscience, 2011:1–14.

Koenig T, Melie-García L (2009) Statistical analysis of multichannel scalp field data. In: Electrical Neuroimaging (Michel CM, Koenig T, Brandeis D, Gianotti LRR, Wackermann J, eds), pp 169–189. New York: Cambridge University Press.

Koenig T, Melie-García L (2010) A method to determine the presence of averaged event-related fields using randomization tests. Brain Topography 23(3):233–242.

Koenig T, Pascual-Marqui RD (2009) Multichannel frequency and time-frequency analysis. In: Electrical Neuroimaging (Michel CM, Koenig T, Brandeis D, Gianotti LRR, Wackermann J, eds), pp 145–168. New York: Cambridge University Press.

Koenig T, Stein M, Grieder M, Kottlow M (2014) A tutorial on data-driven methods for statistically assessing ERP topographies. Brain Topography 27(1):72–83.

Lehmann D, Ozaki H, Pal I (1987) EEG alpha map series: brain micro-states by space oriented adaptive segmentation. Electroencephalography and Clinical Neurophysiology 67(3):271–288.

Lehmann D, Skrandies W (1980) Reference-free identification of components of checkerboard-evoked multichannel potential fields. Electroencephalography and Clinical Neurophysiology 48(6):609–621.

Leiderman EA, Strejilevich SA (2004) Visuospatial deficits in schizophrenia: central executive and memory subsystems impairments. Schizophrenia Research 68:217–223.

Mangun GR, Hillyard SA (1991) Modulations of sensory-evoked brain potentials indicate changes in perceptual processing during visual-spatial priming. Journal of Experimental Psychology: Human Perception and Performance 17(4):1057–1074.

Marshall JC, Fink GR (2001) Spatial cognition: where we were and where we are. NeuroImage 14(1):2–7.

McCourt ME, Shpaner M, Javitt DC, Foxe JJ (2008) Hemispheric asymmetry and callosal integration of visuospatial attention in schizophrenia: A tachistoscopic line bisection study. Schizophr Res 102(1-3):189–196.

Mesulam MM (1999) Spatial attention and neglect: parietal, frontal and cingulate contributions to the mental representation and attentional targeting of salient extrapersonal events. Neuropsychology 354(1387):1325–1346.

Murray MM, Brunet D, Michel CM (2008) Topographic ERP analyses: a step-by-step tutorial review. Brain Topography 20(4):249–264.

Müri RM, Bühler R, Heinemann D, Mosimann UP, Felblinger J, Schlaepfer TE, Hess CW (2002) Hemispheric asymmetry in visuospatial attention assessed with transcranial magnetic stimulation. Experimental Brain Research 143(4):426–430.

Newcombe F, Ratcliff G, Damasio H (1987) Dissociable visual and spatial impairments following right posterior cerebral lesions: clinical, neuropsychological and anatomical evidence. Neuropsychologia 25(1B):149–161.

Oka S, van Tonder G, Ejima Y (2001) A VEP study on visual processing of figural geometry. Vision Research 41:3791–3803.

Oldfield RC (1971) The assessment and analysis of handedness: the Edinburgh inventory. Neuropsychologia 9(1):97–113.

Prvulovic D, Hubl D, Sack AT, Melillo L, Maurer K, Frölich L, Lanfermann H, Zanella FE, Goebel R, Linden DEJ, Dierks T (2002) Functional imaging of visuospatial processing in Alzheimer's disease. NeuroImage 17:1403–1414.

Roser ME, Fiser J, Aslin RN, Gazzaniga MS (2011) Right hemisphere dominance in visual statistical learning. Journal of Cognitive Neuroscience 23(5):1088–1099.

Sack AT, Hubl D, Prvulovic D, Formisano E, Jandl M, Zanella FE, Maurer K, Goebel R, Dierks T, Linden DEJ (2002a) The experimental combination of rTMS and fMRI reveals the functional relevance of parietal cortex for visuospatial functions. Cognitive Brain Research 13(1):85–93.

Sack AT, Kohler A, Bestmann S, Linden DEJ, Dechent P, Goebel R, Baudewig J (2007) Imaging the brain activity changes underlying impaired visuospatial judgments: simultaneous fMRI, TMS, and behavioral studies. Cerebral Cortex 17(12):2841–2852.

Sack AT, Sperling JM, Prvulovic D, Formisano E, Goebel R, Di Salle F, Dierks T, Linden DEJ (2002b) Tracking the mind's image in the brain II: Transcranial magnetic stimulation reveals parietal asymmetry in visuospatial imagery. Neuron 35(1):195–204.

Schechter I, Butler PD, Zemon VM, Revheim N, Saperstein AM, Jalbrzikowski M, Pasternak R, Silipo G, Javitt DC (2005) Impairments in generation of early-stage transient visual evoked potentials to magno- and parvocellular-selective stimuli in schizophrenia. Clin Neurophysiol 116(9):2204–2215.

Schicke T, Muckli L, Beer AL, Wibral M, Singer W, Goebel R, Rösler F, Röder B (2006) Tight covariation of BOLD signal changes and slow ERPs in the parietal cortex in a parametric spatial imagery task with haptic acquisition. European Journal of Neuroscience 23(7):1910–1918.

Shulman GL, Pope DLW, Astafiev SV, McAvoy MP, Snyder AZ, Corbetta M (2010) Right hemisphere dominance during spatial selective attention and target detection occurs

outside the dorsal frontoparietal network. The Journal of Neuroscience 30(10):3640–3651.

Thulborn KR, Martin C, Voyvodic JT (2000) Functional MR imaging using a visually guided saccade paradigm for comparing activation patterns in patients with probable Alzheimer's disease and in cognitively able elderly volunteers. American Journal of Neuroradiology 21(3):524–531.

Trojano L, Grossi D, Linden DEJ, Formisano E, Hacker H, Zanella FE, Goebel R, Di Salle F (2000) Matching two imagined clocks: the functional anatomy of spatial analysis in the absence of visual stimulation. Cerebral Cortex 10(5):473–481.

Vannini P, Almkvist O, Franck A, Jonsson T, Volpe U, Kristoffersen Wiberg M, Wahlund LO, Dierks T (2004). Task demand modulations of visuospatial processing measured with functional magnetic resonance imaging. NeuroImage, 21(1), 58-68.

Vaughan HG (1982) The neural origins of human event-related potentials. Annals of the New York Academy of Sciences 388:125–138.

Zhai J, Zhang Q, Cheng L, Chen M, Wang K, Liu Y, Deng X, Chen X, Shen Q, Xu Z, Ji F, Liu C, Dong Q, Chen C, Li J (2011) Risk variants in the S100B gene, associated with elevated S100B levels, are also associated with visuospatial disability of schizophrenia. Behav Brain Res 217(2):363–368.

Figure captions

Fig. 1. Stimuli and experimental procedure (see Material and Methods for a detailed description). **a)** Example clocks with 30, 120, 60, and 90 degrees between alternating white and yellow clock hands (seen from the upper left to the lower right clock). **b)** Experimental paradigm for one block, starting with the block instruction (either COLOR or ANGLE discrimination).

Fig. 2. Mean RTs and accuracy in a) the Angle task, and b) the Color task for different stimuli. Y – yellow clock hands, W – white clock hands; numbers indicate the angle size between clock hands. Different colors of columns indicate RTs for target and non-target stimuli (see legend).

Fig. 3. Waveshapes of the obtained grand average ERPs for each condition (see color legend) are presented for electrodes PO3, Pz, PO4, O1, Oz, and O2. Black marks on the scalp map (right upper corner, head shown from the top, nose up) indicate positions of presented electrodes. Electrodes are presented in the order corresponding to their positions on the scalp.

Fig. 4. MS analysis results. Different colors are attributed to different MS classes. Color indicates the assignment of time to the specific MS class. The height of the colored area indicates the variance explained by the microstate model, and the black line enclosing the colored areas represents the GFP. Red vertical lines indicate the mean RT in each condition. Dark horizontal error bars crossing the red vertical lines indicate standard deviation from the mean RT (N = 14).

Figure 1

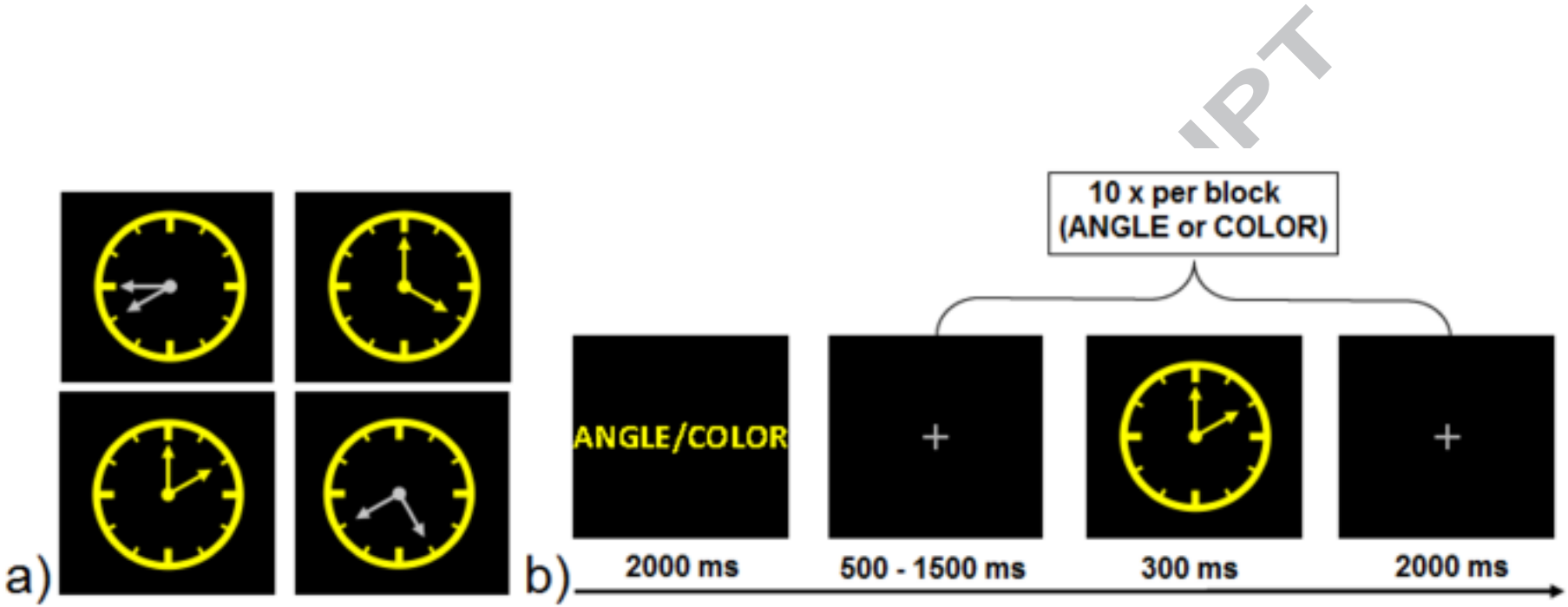

Figure 2

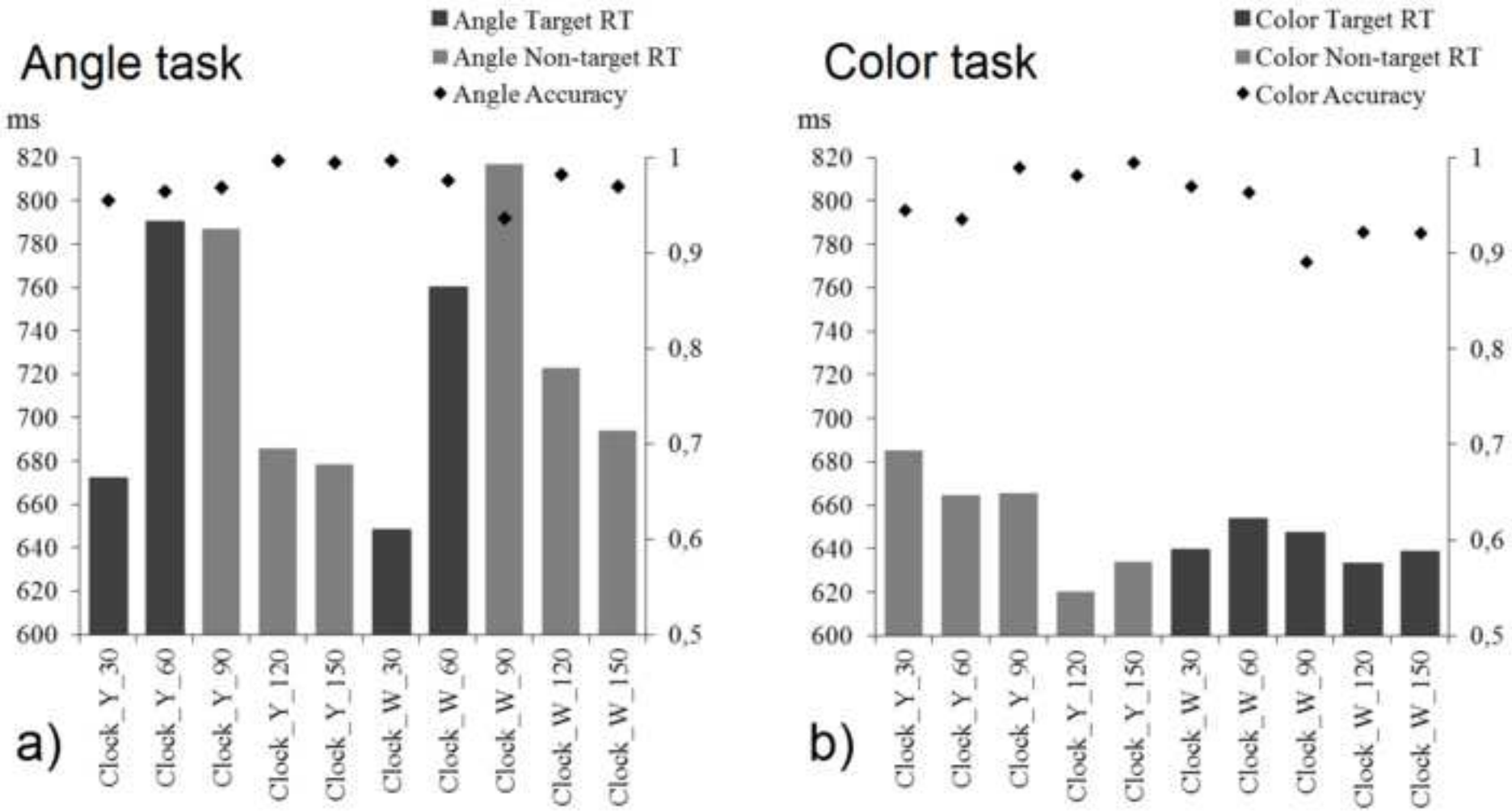

Figure 3

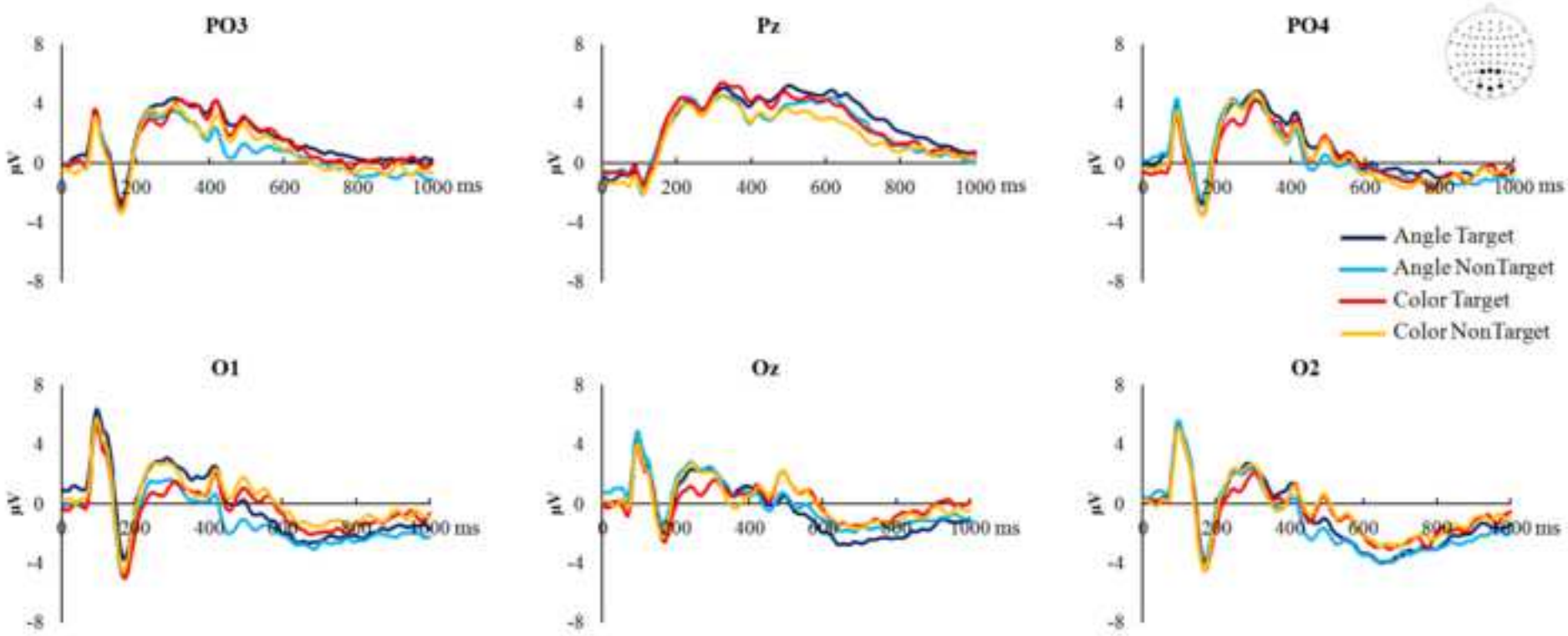

Figure 4

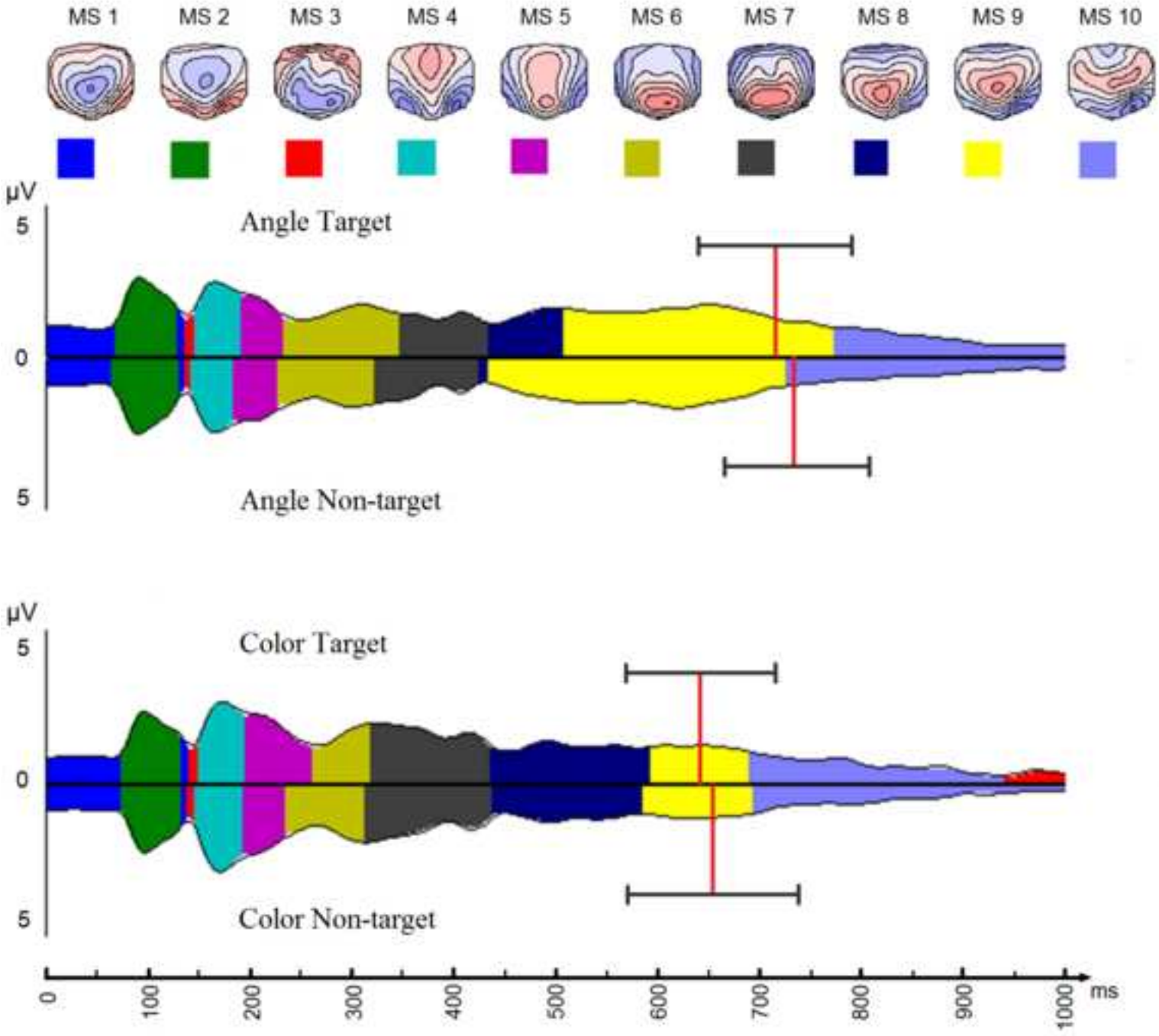

HIGHLIGHTS:

- EEG reveals differential temporal dynamics of network activation in a visuospatial and color-judgment control task.
- During visuospatial judgment and color judgment the same cortical networks get activated.
- Task-specific network activations are mainly characterized by differential timing in later processing stages.
- The described temporal dynamics can serve as a baseline for changes in network activation in clinical conditions.